ELECTRONIC SUPPLEMENTARY INFORMATION

CO_2 Adduct of Lewis Acid-Base Pair ($LBCO_2LA$; LB = PMe_3, NHC and LA = AlH_3, $AlCl_3$, BH_3) – Analogues to Carboxylic Acid and its Derivatives

Indu Purushothaman,[a] Susmita De[*a], Pattiyil Parameswaran[*a]

a Ms. P. Indu, Dr. S. De, Dr. P. Parameswaran
Department of Chemistry, National Institute of Technology Calicut, NIT Calicut Campus P.O., Kozhikode - 673 601, Kerala, India.
E-mail: param@nitc.ac.in, susmitade1980@gmail.com

CONTENTS

Table S3: The optimized Cartesian coordinates and the total bonding energies (in a.u.) including zero point energy correction of all the calculated molecules at the BP86/TZ2P level of theory (E) using ADF 2013.01. Symmetry of the structures is mentioned in the parenthesis. The number of imaginary frequencies is abbreviated as Nimag.

Table S4: Important geometrical parameters of the optimized geometries and the corresponding crystal structures of CO_2 adduct of Lewis acid-base pair, carboxylic acids and esters. Bond lengths are given in angstroms and angles in degrees.

Table S5: EDA-NOCV results for $CH_3COOC_2H_5$ (**10**) and $C_2H_5COOC_3H_7$ **(11)** at the BP86/TZ2P level of theory using ADF 2013.01 package. Energies are in kcal/mol

Table S6: Detail description of different bonding schemes described in Scheme 2.

Table S1 : Energy Decomposition Analysis data of LB–C_{CO2LA} bond (LB = PMe_3, NHC and LA = $AlCl_3$, AlH_3, BH_3) in $PMe_3CO_2AlH_3$ (**1**), $PMe_3CO_2AlCl_3$ (**2**), $PMe_3CO_2BH_3$ (**3**), $NHCCO_2AlH_3$ (**4**), $NHCCO_2AlCl_3$ (**5**), $NHCCO_2BH_3$ (**6**) and R–$C_{CO2R'}$ bond (R, R′ = CH_3, H) in HCOOH (**7**), CH_3COOH (**8**) and CH_3COOCH_3 (**9**) at the BP86/TZ2P level of theory using ADF 2013.01 package. Energies are in kcal/mol.

	1		**2**		**3**		**4**		**5**		**6**		**7**		**8**		**9**	
Bond	P→C	$P^+—C^-$	P→C	$P^+—C^-$	P→C	$P^+—C^-$	C→C	$C^+—C^-$	C→C	$C^+—C^-$	C→C	$C^+–C^-$	$H^-→C^+$	H–C	$C^-→C^+$	C–C	$C^-→C^+$	C–C
ΔE_{int}	-66.4	-162.7	-77.9	-152.8	-61.9	-168.8	-85.8	-196.1	-112.5	-197.2	-89.1	-201.6	-331.9	-107.5	-349.2	-107.3	-332.3	-105.7
ΔE_{Pauli}	243.4	197.3	239.5	193.3	196.6	170.4	397.1	267.4	417.0	277.3	392.2	277.6	297.0	121.6	402.1	264.5	404.86	265.6
ΔE_{elstat} [a]	-136.8	-206.6	-135.1	-195.4	-113.9	-196.2	-222.5	-244.5	-234.2	-243.1	-221.0	-257.3	-301.6	-71.8	-392.6	-159.6	-380.5	-160.5
	(44.2%)	(57.4%)	(42.6%)	(56.5%)	(44.0%)	(57.8%)	(46.1%)	(52.8%)	(44.2%)	(51.2%)	(45.9%)	(53.7%)	(48.0%)	(31.4%)	(52.2%)	(42.9%)	(51.6%)	(43.2%)
ΔE_{orb} [a]	-173.1	-153.5	-182.3	-150.7	-144.7	143.1	-260.4	-219.0	-295.3	-231.4	-260.3	-221.9	-327.3	-157.2	-358.8	-212.3	-356.7	-210.8
	(55.8%)	(42.6%)	(57.4%)	(43.5%)	(56.0%)	(42.2%)	(53.9%)	(47.2%)	(55.8%)	(48.8%)	(54.1%)	(46.3%)	(52.0%)	(68.6%)	(47.8%)	(57.1%)	(48.4%)	(56.7%)
ΔE_{σ} [b]	-144.6	-123.9	-153.3	-122.3	-120.8	-116.3	-213.4	-182.3	-230.7	-179.5	-212.5	-182.3	-318.9	-142.4	-316.1	-185.4	-314.0	-184.8
	(83.5%)	(71.6%)	(84.1%)	(81.2%)	(83.5%)	(81.3%)	(82.0%)	(83.2%)	(78.1%)	(77.6%)	(81.6%)	(82.2%)	(97.4%)	(90.6%)	(88.1%)	(87.3%)	(88.0%)	(87.7%)
ΔE_{π} [b]	-6.0	-6.5	-6.1	-6.1	-5.1	-5.6	-16.4	-12.2	-19.8	-13.5	-16.9	-13.8	-3.3	-10.0	-18.5	-10.5	-16.8	-9.9
	(3.5%)	(3.8%)	(3.3%)	(4.0%)	(3.5%)	(3.9%)	(6.3%)	(5.6%)	(6.7%)	(5.8%)	(6.5%)	(6.2%)	(1.0%)	(6.4%)	(5.2%)	(4.9%)	(4.7%)	(4.7%)
ΔE_{rest} [b,c]	-22.5	-42.7	-22.9	-22.3	-18.8	-21.2	-30.6	-35.5	-44.8	38.4	-30.9	-25.8	-5.1	-4.8	-24.2	-16.4	-25.9	16.1
	(13.0%)	(24.7%)	(12.6%)	(14.8%)	(13.0%)	(14.8%)	(11.8%)	(16.2%)	(15.2%)	(16.6%)	(11.9%)	(11.6%)	(1.6%)	(3.1%)	(6.7%)	(7.7%)	(7.3%)	(7.6%)
ΔE_{prep}	51.8	148.0	56.1	131.0	49.7	156.6	50.4	160.7	59.9	144.6	55.3	167.8	227.5	3.1	254.7	12.8	239.5	13.9
$\Delta E_{(-De)}$	-14.7	-14.7	-21.8	-21.8	-12.2	-12.2	-35.4	-35.4	-52.6	-52.6	-33.8	-33.8	-104.4	-104.4	-94.5	-94.5	-92.8	-92.8
$\Delta E_{orb}/\Delta E_{elstat}$	1.27	0.74	1.35	0.77	1.27	0.73	1.17	0.90	1.26	0.95	1.18	0.86	1.09	2.19	0.91	1.33	0.94	1.31

[a]Values in parenthesis give the percentage contribution to the total attractive interactions $\Delta E_{elstat} + \Delta E_{orb}$

[b]Values in parenthesis give the percentage contribution to orbital interaction ΔE_{orb}

[c]$\Delta E_{\mathbf{rest}} = \Delta E_{\mathbf{orb}} – (\Delta E_{\sigma} + \Delta E_{\pi})$

Table S2: Energy Decomposition Analysis data of $_{LBCO_2}O$–LA bond (LB = PMe_3, NHC and LA = $AlCl_3$, AlH_3, BH_3) in $PMe_3CO_2AlH_3$ (**1**), $PMe_3CO_2AlCl_3$ (**2**), $PMe_3CO_2BH_3$ (**3**), $NHCCO_2AlH_3$ (**4**), $NHCCO_2AlCl_3$ (**5**), $NHCCO_2BH_3$ (**6**) and $_{RCO_2}O$–R′ bond (R, R′ = CH_3, H) in HCOOH (**7**), CH_3COOH (**8**) and CH_3COOCH_3 (**9**) at the BP86/TZ2P level of theory using ADF 2013.01 package. Energies are in kcal/mol.

	1		**2**		**3**		**4**		**5**		**6**		**7**		**8**		**9**	
Bond	O→Al	O^+–Al^-	O→Al	O^+–Al^-	O→B	O^+–B^-	O→Al	O^+–Al^-	O→Al	O^+–Al^-	O→B	O^+–B^-	O^-→H^+	O–H	O^-→H^+	O–H	O^+→C^-	O–C
ΔE_{int}	-39.8	-218.7	-54.2	-211.6	-44.8	-231.3	-36.4	-233.9	-67.3	-233.9	-40.3	-230.8	-356.9	-136.1	-362.2	-117.9	-280.6	-99.2
ΔE_{Pauli}	69.3	209.6	89.7	265.6	109.2	319.5	56.4	181.3	102.0	246.6	97.6	252.3	0.0	287.5	0.0	261.0	189.8	359.4
ΔE_{elstat} [a]	-65.8 (60.4%)	-199.3 (46.5%)	-85.5 (59.4%)	-214.8 (45.0%)	-73.5 (47.7%)	-251.7 (45.7%)	-57.9 (62.5%)	-179.0 (43.1%)	-93.7 (55.4%)	-208.0 (43.3%)	-65.4 (47.4%)	-212.7 (44.0%)	-182.9 (51.2%)	-116.5 (27.5%)	-183.7 (50.7%)	-95.8 (25.3%)	-248.9 (52.9%)	-159.8 (34.8%)
ΔE_{orb} [a]	-43.2 (39.6%)	-228.9 (53.5%)	-58.4 (40.6%)	-262.4 (55.0%)	-80.5 (52.3%)	-299.1 (54.3%)	-34.8 (37.5%)	-236.2 (56.9%)	-75.6 (44.6%)	-272.6 (56.7%)	-72.5 (52.6%)	-270.4 (56.0%)	-174.0 (48.8%)	-307.1 (72.5%)	-178.5 (49.3%)	-283.1 (74.7%)	-221.4 (47.1%)	-298.9 (65.2%)
ΔE_{σ} [b]	-22.7 (52.5%)	-211.5 (92.4%)	-29.2 (50.0%)	-244.0 (93.0%)	-60.1 (74.7%)	-278.9 (93.2%)	-21.2 (60.9%)	-225.9 (95.6%)	-31.0 (41.0%)	-245.3 (90.0%)	-56.0 (77.2%)	-251.4 (93.0%)	-127.7 (73.4%)	-295.5 (96.2%)	-129.2 (72.4%)	-271.6 (95.9%)	-174.8 (79.0%)	-279.9 (93.6%)
ΔE_{π} [b]	-5.7 (13.9%)	-3.4 (1.5%)	-9.7 (16.6%)	-4.5 (1.7%)	-4.8 (6.0%)	-2.8 (0.01%)	-4.4 (12.6%)	-3.7 (1.6%)	-12.0 (15.9%)	-6.8 (2.5%)	-4.8 (6.6%)	-8.3 (3.1%)	-22.8 (13.1%)	-6.4 (2.1%)	-23.0 (12.9%)	-4.9 (1.7%)	-18.0 (8.1%)	-7.7 (2.6%)
ΔE_{rest} [b,c]	-14.8 (34.3%)	-14.0 (6.1%)	-19.5 (33.4%)	-13.9 (5.3%)	-15.6 (19.4%)	-17.4 (5.8%)	-9.2 (26.4%)	-6.6 (2.8%)	-32.6 (43.1%)	-20.5 (7.5%)	-11.7 (16.1%)	-10.7 (3.9%)	-23.5 (13.5%)	-5.2 (1.7%)	-26.3 (14.7%)	-6.6 (2.3%)	-28.6 (12.9%)	-11.3 (3.8%)
ΔE_{prep}	22.5	201.4	28.8	186.2	32.3	218.8	7.5	205.0	20.6	187.3	15.7	206.3	245.6	24.7	254.6	10.3	199.4	18.1
$\Delta E_{(-D_e)}$	-17.3	-17.3	-25.4	-25.4	-12.5	-12.5	-28.9	-28.9	-46.7	-46.7	-24.5	-24.5	-111.3	-111.3	-107.6	-107.6	-81.1	-81.1
$\Delta E_{orb}/\Delta E_{elstat}$	0.65	1.15	0.68	1.22	1.09	1.19	0.60	1.32	0.81	1.31	1.11	1.27	0.95	2.64	0.97	2.95	0.89	1.87

[a] Values in parenthesis give the percentage contribution to the total attractive interactions $\Delta E_{elstat} + \Delta E_{orb}$

[b] Values in parenthesis give the percentage contribution to orbital interaction ΔE_{orb}

[c] $\Delta E_{\mathbf{rest}} = \Delta E_{\mathbf{orb}} - (\Delta E_{\sigma} + \Delta E_{\pi})$

$PMe_3CO_2AlH_3$ (1)

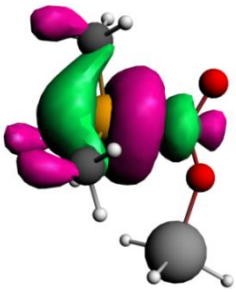

Ψ_{-1}(-0.51)

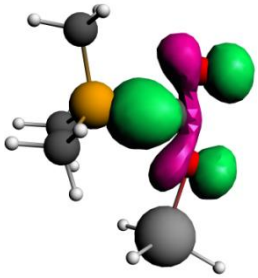

Ψ_1(0.51)

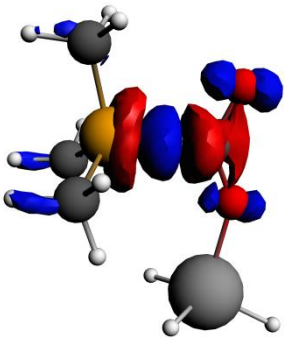

$\Delta\rho_1$(ΔE=-123.9 kcal/mol)

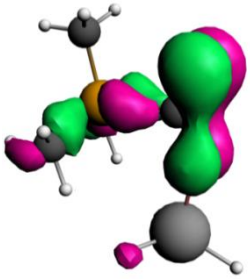

Ψ_{-2}(-0.10)

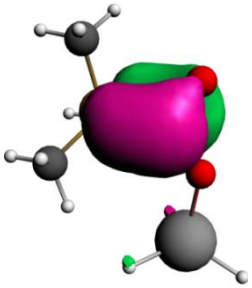

Ψ_2(0.10)

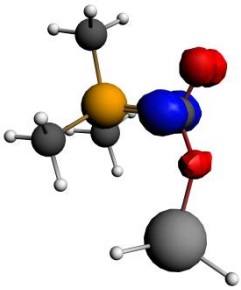

$\Delta\rho_2$(ΔE=-6.5 kcal/mol)

$PMe_3CO_2AlCl_3$ (2)

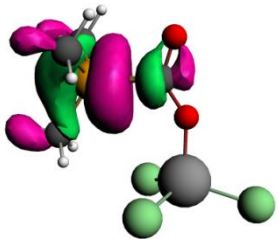

Ψ_{-1}(-0.53)

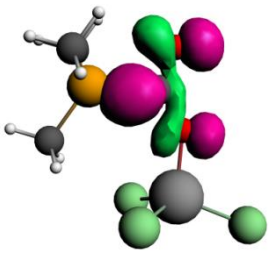

Ψ_1(0.53)

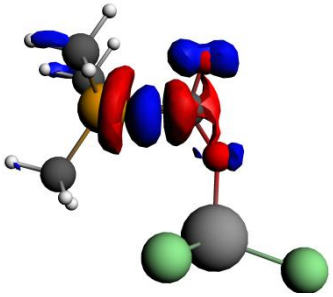

$\Delta\rho_1$(ΔE=-122.3 kcal/mol)

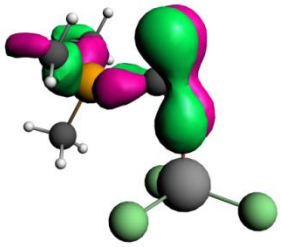

Ψ_{-3}(-0.09)

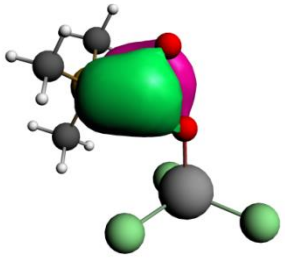

Ψ_3(0.09)

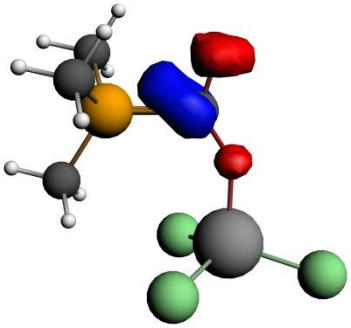

$\Delta\rho_3$(ΔE=-6.1 kcal/mol)

Figure S1 (Contd.)

$PMe_3CO_2BH_3$ (3)

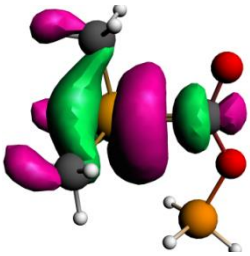

Ψ_{-1}(-0.48)

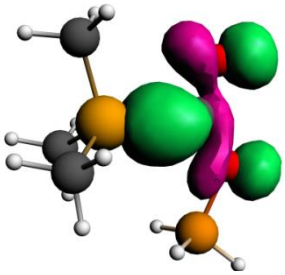

Ψ_1(0.48)

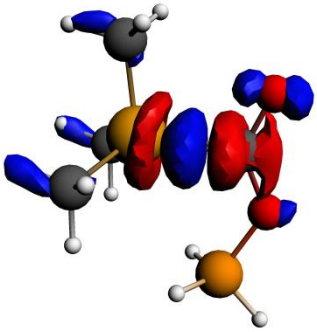

$\Delta\rho_1$(ΔE=-116.3 kcal/mol)

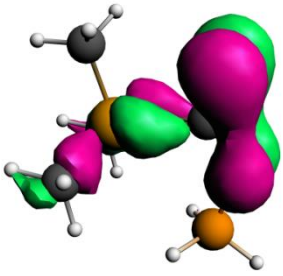

Ψ_{-3}(-0.09)

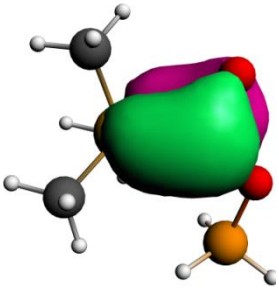

Ψ_3(0.09)

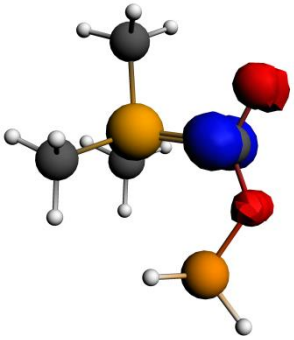

$\Delta\rho_3$(ΔE=-5.6 kcal/mol)

$NHCCO_2AlH_3$ (4)

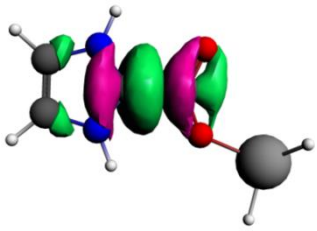

Ψ_{-1}(-0.48)

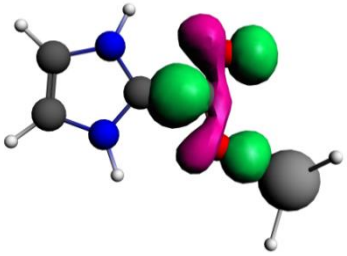

Ψ_1(0.48)

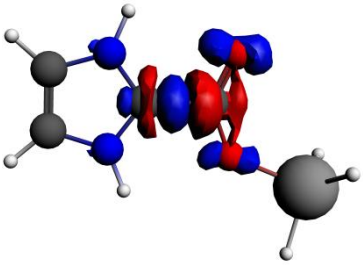

$\Delta\rho_1$(ΔE=-182.3 kcal/mol)

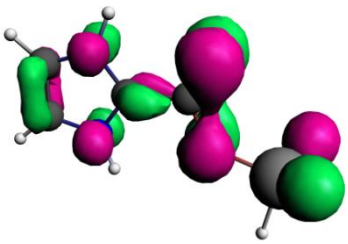

Ψ_{-2}(-0.16)

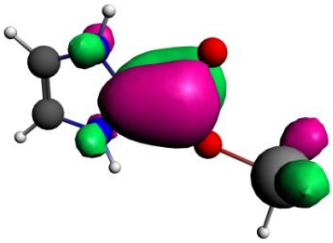

Ψ_2(0.16)

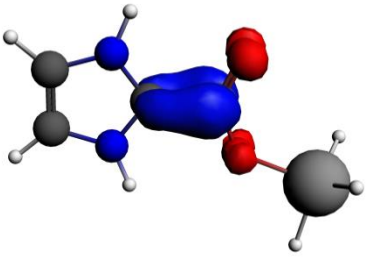

$\Delta\rho_2$(ΔE=-12.2 kcal/mol)

Figure S1 (Contd.)

NHCCO$_2$AlCl$_3$ (5)

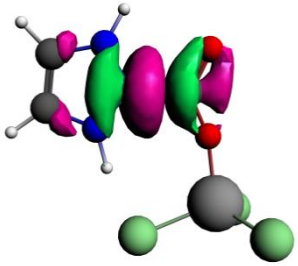

Ψ_{-1}(-0.50)

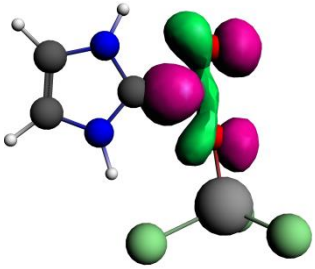

Ψ_1(0.50)

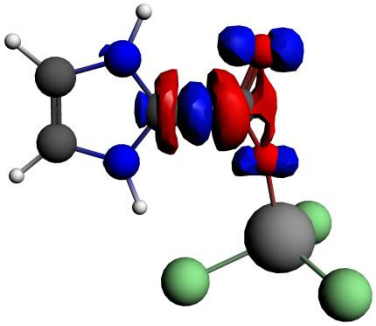

$\Delta\rho_1$(ΔE=-179.5 kcal/mol)

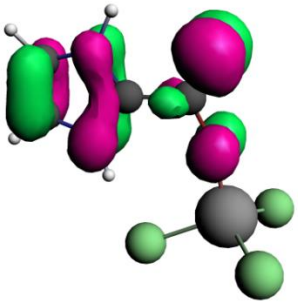

Ψ_{-2}(-0.15)

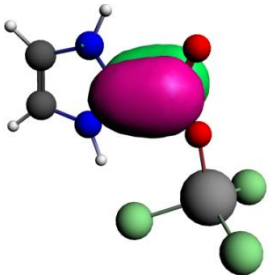

Ψ_2(0.15)

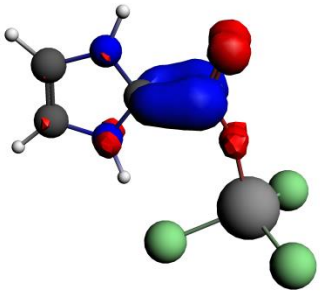

$\Delta\rho_2$(ΔE=-13.5 kcal/mol)

NHCCO$_2$BH$_3$ (6)

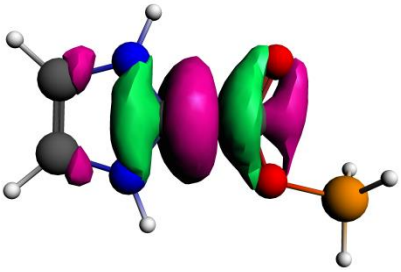

Ψ_{-1}(-0.48)

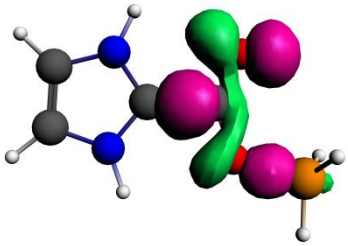

Ψ_1(0.48)

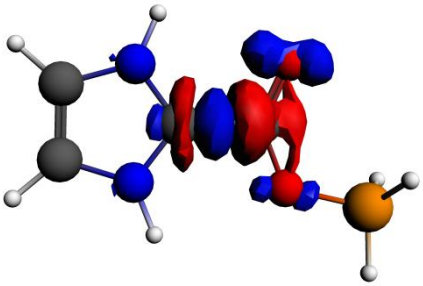

$\Delta\rho_1$(ΔE=-182.3 kcal/mol)

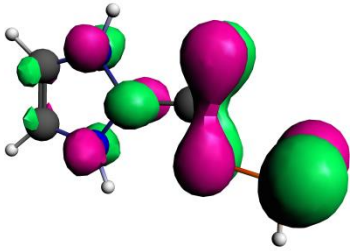

Ψ_{-2}(-0.20)

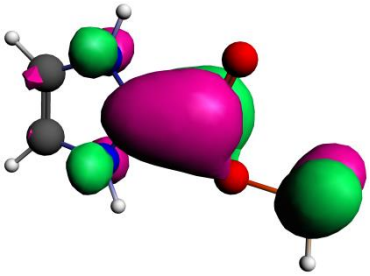

Ψ_2(0.20)

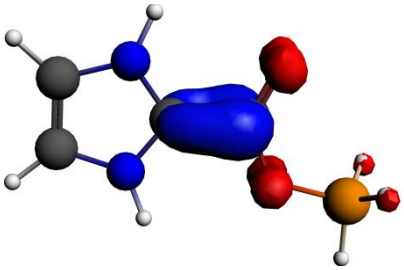

$\Delta\rho_2$(ΔE=-13.8 kcal/mol)

Figure S1 (Contd.)

HCOOH (7)

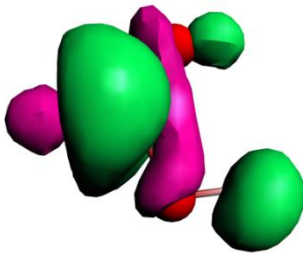

Ψ_{-1}(-0.34)

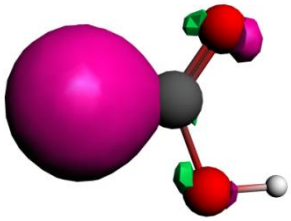

Ψ_{1}(0.34)

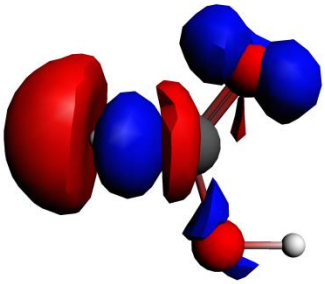

$\Delta\rho_1$(ΔE=-142.4 kcal/mol)

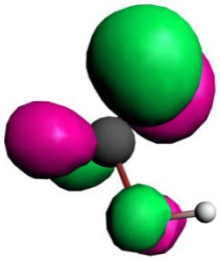

Ψ_{-2}(-0.06)

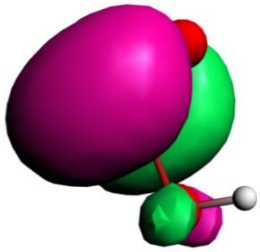

Ψ_{2}(0.06)

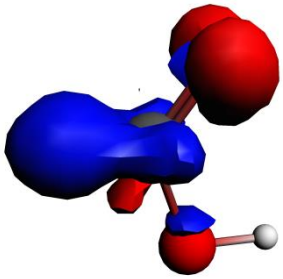

$\Delta\rho_2$(ΔE=-10.0 kcal/mol)

CH_3COOH (8)

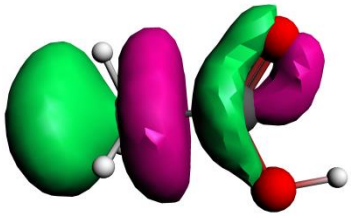

Ψ_{-1}(-0.57)

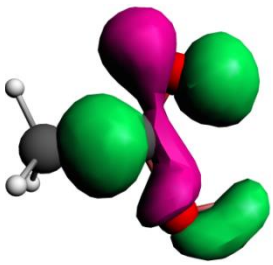

Ψ_{1}(0.57)

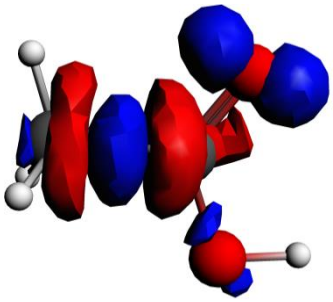

$\Delta\rho_1$(ΔE=-185.4 kcal/mol)

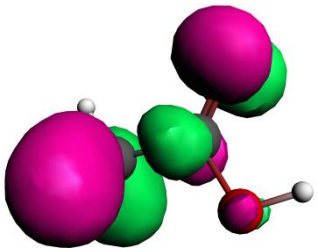

Ψ_{-2}(-0.13)

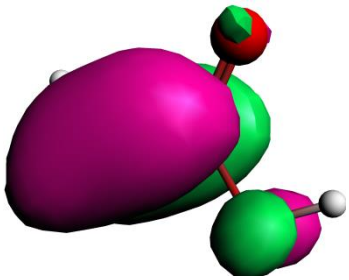

Ψ_{2}(0.13)

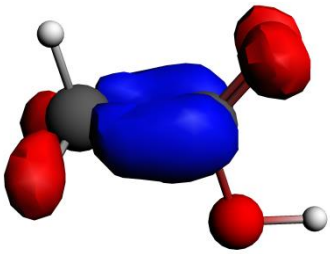

$\Delta\rho_2$(ΔE=-10.5 kcal/mol)

Figure S1 (Contd.)

CH_3COOCH_3 (9)

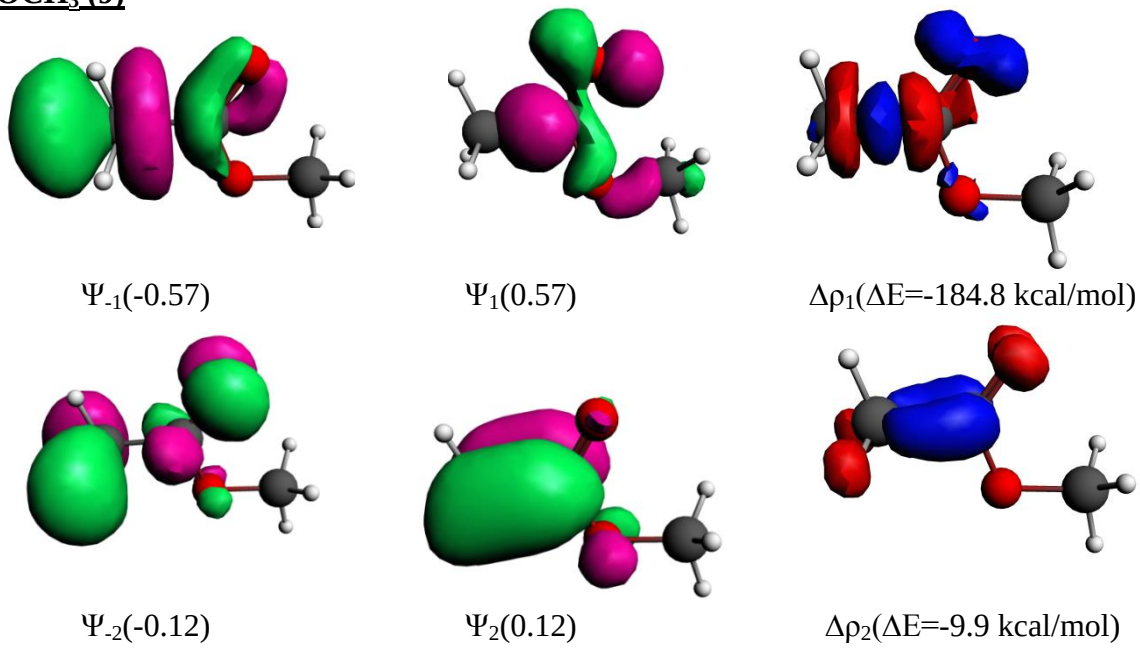

Figure S1: The α-NOCV pair of orbitals Ψ_{-1}/ Ψ_1 and Ψ_{-2}/ Ψ_2 with their eigen values in parenthesis, the associated deformation density plots $\Delta\rho_1$ and $\Delta\rho_2$ and orbital stabilization energies ΔE for the LB–C_{CO_2LA} bond (LB = PMe_3, NHC and LA = $AlCl_3$, AlH_3, BH_3) in $PMe_3CO_2AlH_3$ (**1**), $PMe_3CO_2AlCl_3$ (**2**), $PMe_3CO_2BH_3$ (**3**), $NHCCO_2AlH_3$ (**4**), $NHCCO_2AlCl_3$ (**5**), $NHCCO_2BH_3$ (**6**) and R–$C_{CO_2R'}$ bond (R, R′ = CH_3, H) in HCOOH (**7**), CH_3COOH (**8**) and CH_3COOCH_3 (**9**) at the BP86/TZ2P level of theory using ADF 2013.01 package. The direction of the charge flow in the deformation density plot Δρ is from red → blue. Isosurface value for the α-NOCV pair of orbitals is 0.04 and that for the deformation density is 0.003.

$PMe_3CO_2AlH_3$ (1)

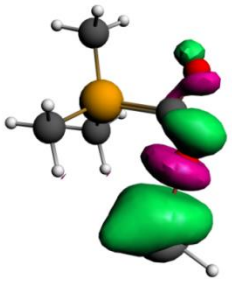

Ψ_{-1}(-0.35)

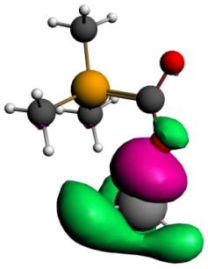

Ψ_1(0.35)

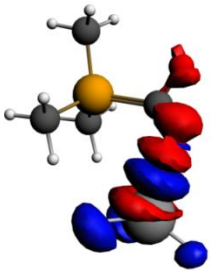

$\Delta\rho_1$(ΔE=-22.7 kcal/mol)

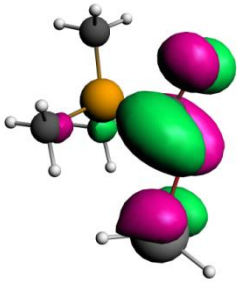

Ψ_{-2}(-0.18)

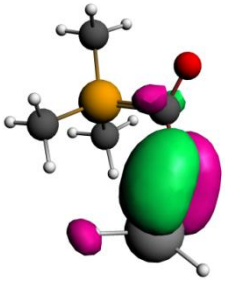

Ψ_2(0.18)

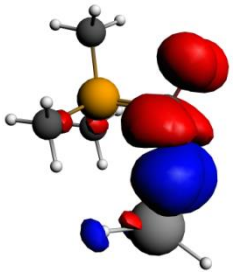

$\Delta\rho_2$(ΔE=-5.7 kcal/mol)

$PMe_3CO_2AlCl_3$ (2)

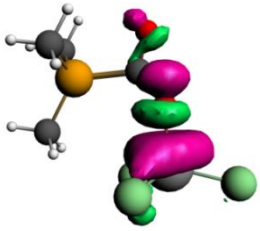

Ψ_{-1}(-0.40)

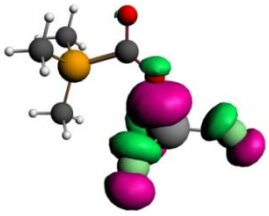

Ψ_1(0.40)

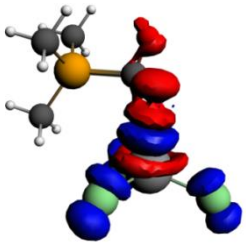

$\Delta\rho_1$(ΔE=-29.2 kcal/mol)

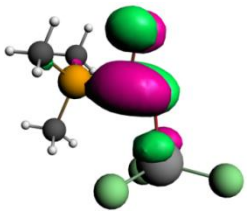

Ψ_{-2}(-0.24)

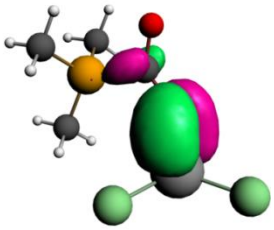

Ψ_2(0.24)

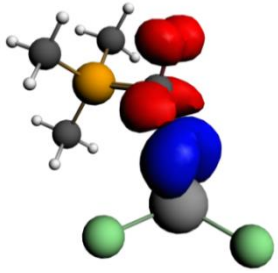

$\Delta\rho_2$(ΔE=-9.7 kcal/mol)

Figure S2 (Contd.)

$PMe_3CO_2BH_3$ (3)

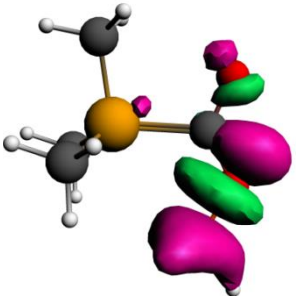

Ψ_{-1}(-0.54)

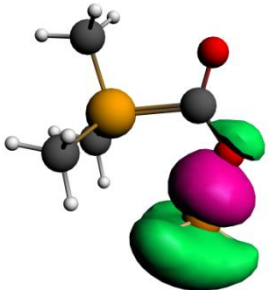

Ψ_1(0.54)

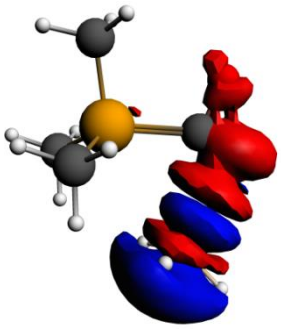

$\Delta\rho_1$(ΔE=-60.1 kcal/mol)

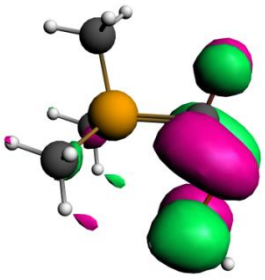

Ψ_{-3}(-0.19)

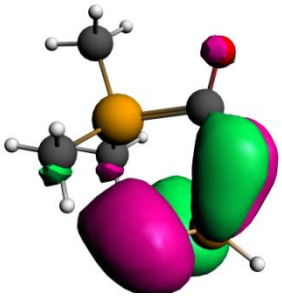

Ψ_2(0.19)

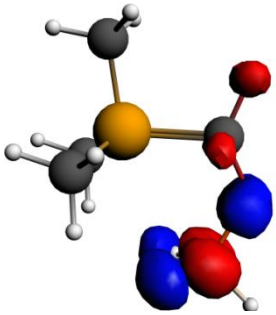

$\Delta\rho_3$(ΔE=-4.8 kcal/mol)

$NHCCO_2AlH_3$ (4)

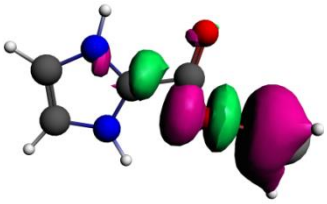

Ψ_{-1}(-0.34)

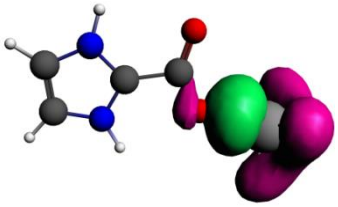

Ψ_1(0.34)

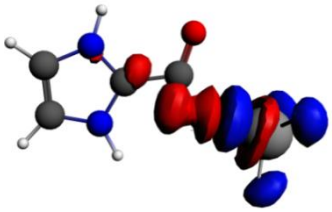

$\Delta\rho_1$(ΔE=-21.2 kcal/mol)

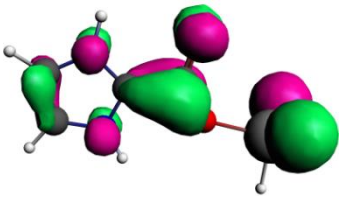

Ψ_{-2}(-0.25)

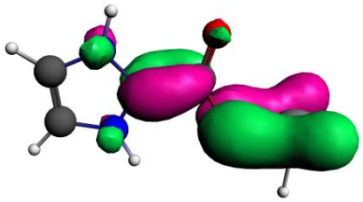

Ψ_2(0.25)

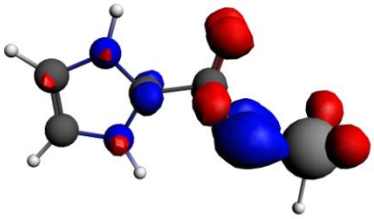

$\Delta\rho_2$(ΔE=-4.4 kcal/mol)

Figure S2 (Contd.)

NHCCO$_2$AlCl$_3$ (5)

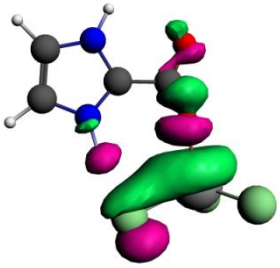

Ψ_{-1}(-0.42)

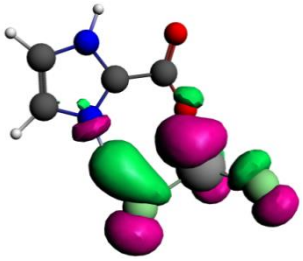

Ψ_1(0.42)

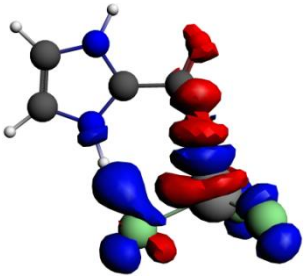

$\Delta\rho_1$(ΔE=-31.0 kcal/mol)

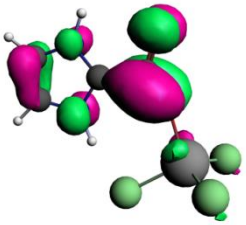

Ψ_{-2}(-0.30)

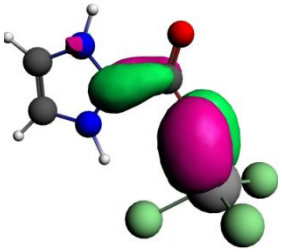

Ψ_2(0.30)

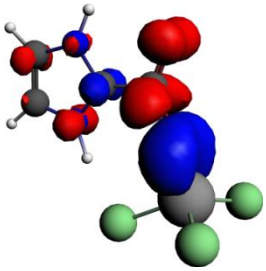

$\Delta\rho_2$(ΔE=-12.0 kcal/mol)

NHCCO$_2$BH$_3$ (6)

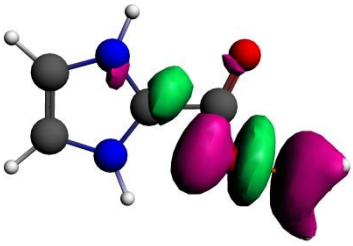

Ψ_{-1}(-0.52)

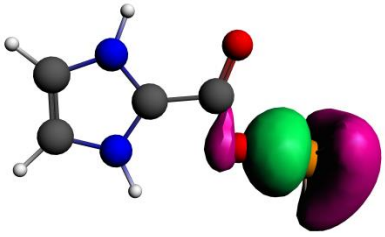

Ψ_1(0.52)

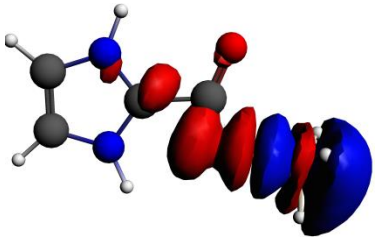

$\Delta\rho_1$(ΔE=-56.0 kcal/mol)

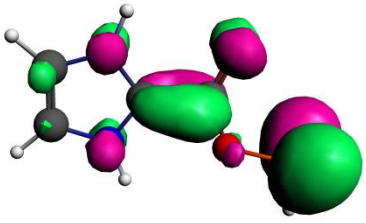

Ψ_{-2}(-0.34)

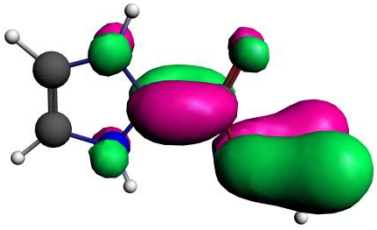

Ψ_2(0.34)

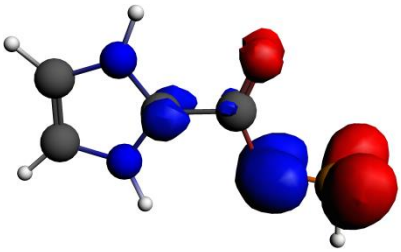

$\Delta\rho_2$(ΔE=-4.8 kcal/mol)

Figure S2 (Contd.)

HCOOH (7)

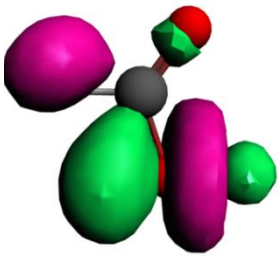

Ψ_{-1}(-0.59)

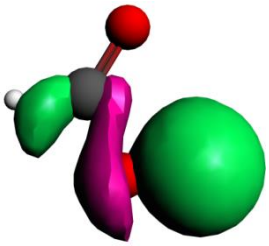

Ψ_{1}(0.59)

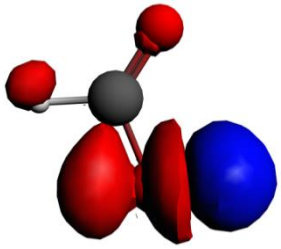

$\Delta\rho_1$(ΔE=-127.7 kcal/mol)

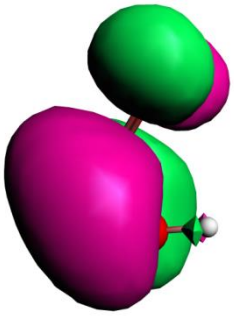

Ψ_{-2}(-0.30)

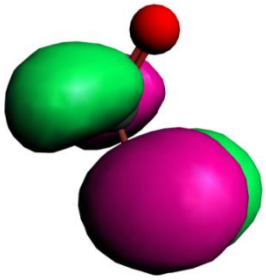

Ψ_{2}(0.30)

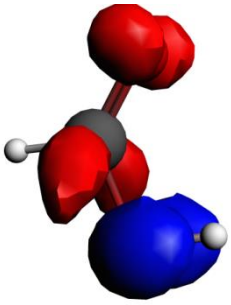

$\Delta\rho_2$(ΔE=-22.8 kcal/mol)

CH_3COOH (8)

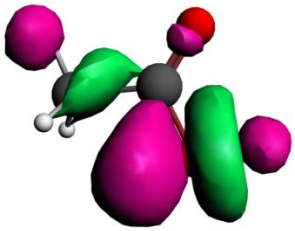

Ψ_{-1}(-0.60)

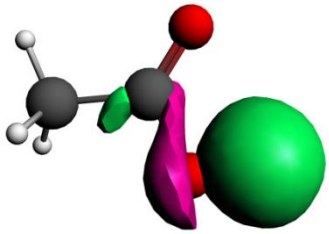

Ψ_{1}(0.60)

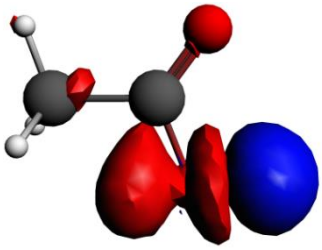

$\Delta\rho_1$(ΔE=-129.2 kcal/mol)

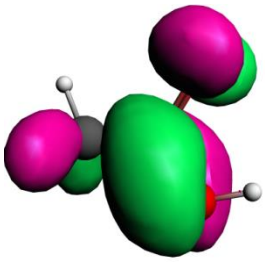

Ψ_{-2}(-0.30)

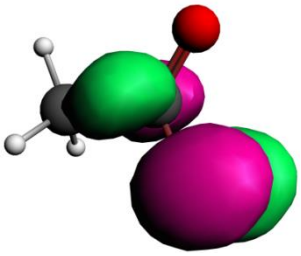

Ψ_{2}(0.30)

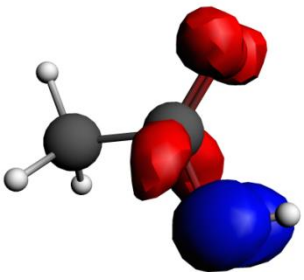

$\Delta\rho_2$(ΔE=-23.01 kcal/mol)

Figure S2 (Contd.)

CH_3COOCH_3 (9)

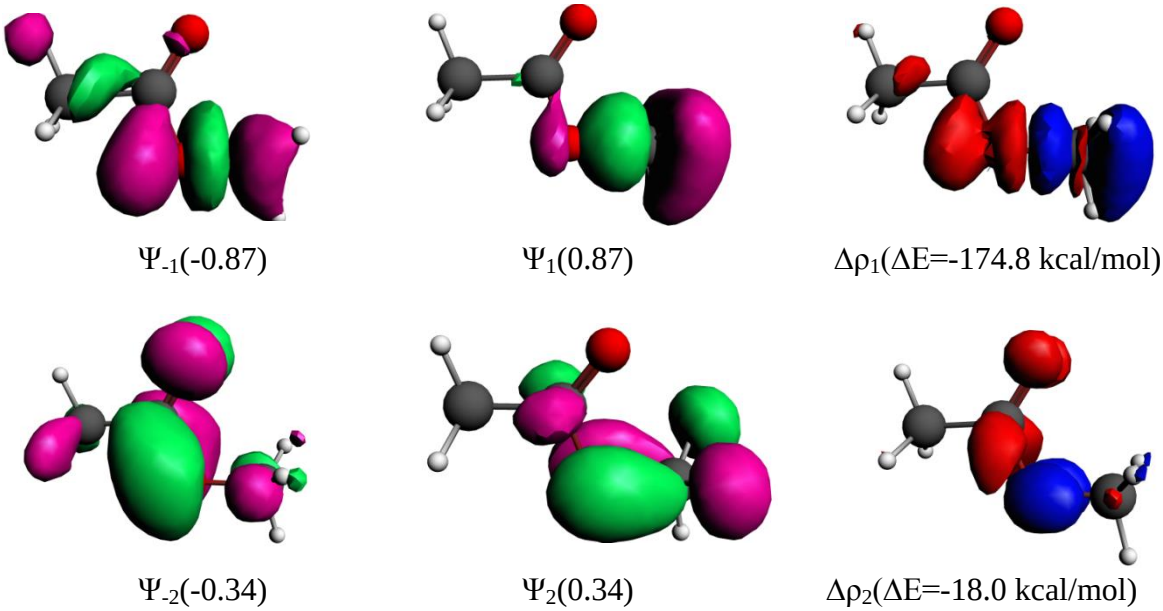

Figure S2: The α-NOCV pair of orbitals Ψ_{-1}/ Ψ_1 and Ψ_{-2}/ Ψ_2 with their eigen values in parenthesis, the associated deformation density plots $\Delta\rho_1$ and $\Delta\rho_2$ and orbital stabilization energies ΔE for the $_{LBCO_2}$O–LA bond (LB = PMe_3, NHC and LA = $AlCl_3$, AlH_3, BH_3) in $PMe_3CO_2AlH_3$ (**1**), $PMe_3CO_2AlCl_3$ (**2**), $PMe_3CO_2BH_3$ (**3**), $NHCCO_2AlH_3$ (**4**), $NHCCO_2AlCl_3$ (**5**), $NHCCO_2BH_3$ (**6**) and $_{RCO_2}$O–R′ bond (R, R′ = CH_3, H) in HCOOH (**7**), CH_3COOH (**8**) and CH_3COOCH_3 (**9**) at the BP86/TZ2P level of theory using ADF 2013.01 package. The direction of the charge flow in the deformation density plot Δρ is from red → blue. Isosurface value for the α-NOCV pair of orbitals is 0.04 and that for the deformation density is 0.003.

Table S3: The optimized Cartesian coordinates and the total bonding energies (in a.u.) including zero point energy correction of all the calculated molecules at the BP86/TZ2P level of theory (E) using ADF 2013.01. Symmetry of the structures is mentioned in the parenthesis. The number of imaginary frequencies is abbreviated as Nimag.

$PMe_3CO_2AlH_3$ (1) (C_1)

E= -3.563608
Nimag=0

15	1.050934000	0.149399000	0.091205000
6	2.459531000	-0.997076000	-0.060242000
1	2.363569000	-1.568401000	-0.993672000
1	3.407749000	-0.442013000	-0.065797000
1	2.428526000	-1.697458000	0.782994000
6	1.301684000	1.133287000	1.602591000
1	2.268318000	1.654967000	1.561966000
1	0.476932000	1.854921000	1.678049000
1	1.281058000	0.455792000	2.467052000
6	1.088377000	1.242956000	-1.366660000
1	0.922848000	0.645294000	-2.273272000
1	0.285665000	1.986382000	-1.278185000
1	2.069824000	1.736977000	-1.422481000
6	-0.490320000	-1.043391000	0.384781000
8	-0.134163000	-2.012065000	1.035184000
8	-1.611370000	-0.708030000	-0.096663000
13	-2.405262000	0.985838000	-0.487767000
1	-2.239025000	1.149085000	-2.085559000
1	-3.880002000	0.903243000	0.130064000
1	-1.356388000	1.946213000	0.321716000

$PMe_3CO_2AlCl_3$ (2) (C_s)

E= -3.659032
Nimag=0

15	-0.946314000	1.322650000	0.000000000
6	0.424202000	-0.056519000	0.000000000
8	-0.142040000	-1.136422000	0.000000000
8	1.663948000	0.223481000	0.000000000
13	2.912215000	1.565786000	0.000000000
17	2.476395000	2.691212000	-1.793602000
17	2.476395000	2.691212000	1.793602000
17	4.814910000	0.636732000	0.000000000
6	-0.554620000	3.095002000	0.000000000
6	-1.933323000	0.944718000	-1.480057000
6	-1.933323000	0.944718000	1.480057000
1	0.043986000	3.337414000	-0.889407000
1	0.043986000	3.337414000	0.889407000
1	-1.496878000	3.662723000	0.000000000
1	-2.863225000	1.529565000	-1.475906000
1	-1.346809000	1.197015000	-2.374299000
1	-2.158455000	-0.128968000	-1.483669000
1	-2.863225000	1.529565000	1.475906000
1	-1.346809000	1.197015000	2.374299000
1	-2.158455000	-0.128968000	1.483669000

$PMe_3CO_2BH_3$ (3) (C_1)

E= -3.311025
Nimag=1; 33.6i

6	0.903932000	0.120765000	0.052532000
7	2.011548000	0.873289000	0.079913000
6	3.134894000	0.076081000	0.000220000
6	2.688042000	-1.214530000	-0.078408000
7	1.310362000	-1.152876000	-0.044113000
1	1.947234000	1.887376000	0.150280000
1	4.139513000	0.475165000	0.005432000
1	3.232335000	-2.145704000	-0.154569000
1	0.633752000	-1.913780000	-0.084970000
6	-0.518590000	0.636240000	0.114790000
8	-1.339407000	-0.344451000	0.063860000
8	-0.648411000	1.854304000	0.199039000
13	-3.275526000	-0.462310000	0.029249000
1	-3.732182000	0.134742000	1.458726000
1	-3.385523000	-2.072015000	-0.119542000
1	-3.690857000	0.391426000	-1.277549000

$NHCCO_2AlH_3$ (4) (C_1)

E= -3.423262
Nimag=1; 9.9i

6	2.329926000	0.205848000	-0.087109000
7	3.618613000	0.471663000	0.184104000
6	4.319156000	-0.698783000	0.349129000
6	3.415181000	-1.712708000	0.167799000
7	2.200973000	-1.126688000	-0.099280000
1	3.946917000	1.434539000	0.236770000
1	5.375710000	-0.722349000	0.577082000
1	3.543235000	-2.785921000	0.208112000
1	1.283129000	-1.610112000	-0.313208000
6	1.326094000	1.312461000	-0.320929000
8	0.105277000	0.945737000	-0.523409000
8	1.795059000	2.442783000	-0.320911000
13	-1.212028000	-0.175049000	0.015810000
17	-1.080563000	-0.245518000	2.148931000
17	-0.591461000	-2.145944000	-0.788336000
17	-3.043907000	0.444277000	-0.841083000

$NHCCO_2AlCl_3$ (5) (C_1)

E= -3.675377
Nimag=0

15	0.884687000	0.199367000	-0.042807000
6	2.383880000	-0.857388000	-0.003352000
1	2.352246000	-1.572349000	-0.833171000
1	3.288781000	-0.237889000	-0.068047000
1	2.399180000	-1.431785000	0.932440000
6	1.133959000	1.311945000	1.393278000
1	2.191443000	1.611966000	1.435424000
1	0.478081000	2.185125000	1.316257000
1	0.875790000	0.762243000	2.309538000
6	1.056897000	1.117254000	-1.618400000
1	0.949745000	0.400200000	-2.445323000
1	0.278670000	1.883989000	-1.701592000
1	2.057185000	1.572278000	-1.665679000
6	-0.507522000	-1.223555000	-0.067557000
8	-0.066453000	-2.328315000	-0.316575000
8	-1.697945000	-0.828007000	0.163457000
5	-2.048188000	0.671299000	0.331767000
1	-1.023861000	1.279339000	-0.009631000
1	-2.939583000	0.935262000	-0.444474000
1	-2.306920000	0.887087000	1.497089000

$NHCCO_2BH_3$ (6) (C_s)

E= -3.420604
Nimag=0

6	0.849571000	0.059897000	0.000000000
7	1.919329000	0.867686000	0.000000000
6	3.082924000	0.124331000	0.000000000
6	2.702671000	-1.188942000	0.000000000
7	1.322117000	-1.196667000	0.000000000
1	1.798824000	1.879224000	0.000000000
1	4.066044000	0.573405000	0.000000000
1	3.294483000	-2.093883000	0.000000000
1	0.686755000	-1.991933000	0.000000000
6	-0.578657000	0.527918000	0.000000000
8	-1.358221000	-0.496764000	0.000000000
8	-0.760098000	1.743257000	0.000000000
5	-2.947986000	-0.384802000	0.000000000
1	-3.257080000	0.232725000	1.005919000
1	-3.311480000	-1.544231000	0.000000000
1	-3.257080000	0.232725000	-1.005919000

HCOOH (7) (C_s)

E= -1.059665
Nimag=0

1	1.028100000	-1.097000000	0.000000000
8	1.143800000	-0.122900000	0.000000000
8	-1.133400000	-0.213000000	0.000000000
6	-0.102200000	0.414200000	0.000000000
1	-0.023700000	1.517000000	0.000000000

CH_3COOH (8) (C_s)

E= -1.643108
Nimag=0

1	-0.967100000	-1.591500000	0.000000000
8	-0.033800000	-1.296000000	0.000000000
8	-1.129800000	0.686700000	0.000000000
6	-0.082900000	0.073200000	0.000000000
6	1.300300000	0.670300000	0.000000000
1	1.854400000	0.327400000	-0.883900000
1	1.228000000	1.760400000	0.000000000
1	1.854400000	0.327400000	0.883900000

CH_3COOCH_3 (9) (C_1)

E= -2.200574
Nimag=1; 14.8i

8	-0.647394000	0.718427000	0.000043000
8	0.355893000	-1.320118000	-0.000057000
6	1.717890000	0.690904000	-0.000077000
6	0.436983000	-0.108378000	0.000003000
6	-1.925238000	0.043693000	-0.000110000
1	1.755939000	1.342390000	0.883096000
1	1.756968000	1.340199000	-0.884828000
1	2.571087000	0.007974000	0.001167000
1	-2.027679000	-0.585927000	-0.892024000
1	-2.675509000	0.838657000	-0.000006000
1	-2.027741000	-0.586220000	0.891592000

$CH_3COOC_2H_5$ (10) (C_1)

E= -2.890096
Nimag=1; 34.7i

8	-0.198304000	0.505703000	-0.069730000
8	1.066906000	-1.327844000	0.386309000
6	2.151342000	0.763738000	-0.190943000
6	0.982740000	-0.157181000	0.070896000
6	-1.392398000	-0.283231000	0.203022000
1	2.332748000	1.371525000	0.706835000
1	1.940568000	1.449373000	-1.019490000
1	3.044096000	0.167076000	-0.397689000
1	-1.382652000	-1.167327000	-0.447963000
1	-1.346607000	-0.635990000	1.242294000
6	-2.596327000	0.601960000	-0.047589000
1	-2.623413000	0.945875000	-1.089869000
1	-3.516898000	0.037015000	0.152563000
1	-2.583311000	1.482151000	0.608514000

$C_2H_5COOC_3H_7$ (11) (C_1)

E= -4.086787
Nimag=0

8	0.151851000	-0.513247000	-0.043557000
8	-1.137623000	1.342377000	-0.302625000
6	-2.192916000	-0.841828000	-0.081425000
6	-1.038222000	0.140203000	-0.153274000
6	1.339914000	0.319911000	-0.139567000

1	-1.983677000	-1.559486000	0.724763000
1	-2.165115000	-1.430157000	-1.013008000
1	1.394736000	0.737967000	-1.155595000
1	1.241509000	1.161286000	0.560122000
6	2.545654000	-0.546989000	0.180548000
1	2.566702000	-1.403065000	-0.510262000
1	2.425949000	-0.960237000	1.193244000
6	-3.549818000	-0.163686000	0.095100000
1	-3.596319000	0.384649000	1.044802000
1	-3.735236000	0.557339000	-0.709892000
1	-4.354729000	-0.909934000	0.089237000
6	3.854511000	0.244163000	0.082744000
1	4.013246000	0.632438000	-0.933940000
1	3.856434000	1.102890000	0.770590000
1	4.715555000	-0.387779000	0.335931000

Table S4: Important geometrical parameters of the optimized geometries and the corresponding crystal structures of CO_2 adduct of Lewis acid-base pair (**A**) and carboxylic acids and esters (**B**). Bond lengths are given in angstroms and angles in degrees. Mean Absloute Deviation (MAD) of the bond lengths are also given.[a]

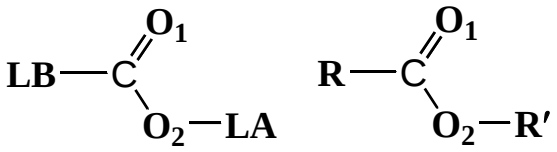

(A) **(B)**

Compound	$Me_3PCO_2AlH_3$ (**1**)	$Me_3PCO_2AlCl_3$ (**2**)	$tBu_3PCO_2Al[OC(CF_3)_3]_3$[5h]		$tBu_3PCO_2Al(C_6F_5)_3$[5g]
P–C	1.971	1.944	1.889		1.883
C–O1	1.220	1.219	1.188		1.211
C–O2	1.265	1.271	1.299		1.288
O2–Al	1.911	1.833	1.790		1.826
O1–C–O2	132.2	130.4	128.9		126.1
MAD	0.059	0.031			
Compound	$Me_3PCO_2BH_3$ (**3**)	$Me_3PCO_2B(C_6F_5)_3$[5c]		$NHCCO_2BH_3$ (**6**)	$R^1{}_2$-$NHCCO_2B(C_6F_5)_3$[5i] (R^1 = *t*-Bu)
P–C	1.991	1.893	C–C	1.503	1.516
C–O1	1.215	1.208	C–O1	1.229	1.202
C–O2	1.276	1.299	C–O2	1.287	1.297
O2–B	1.549	1.547	O2–B	1.594	1.535
O1–C–O2	131.1	127.6	O1–C–O2	134.2	130.1
MAD	0.032			0.027	
Compound	HCO_2H (**7**)[b]		CH_3CO_2H(**8**)[c]		
	Optimized structure	Crystal structure		Optimized Structure	Crystal structure
C–O1	1.207	1.188	C–C	1.507	1.502
C–O2	1.357	1.375	C–O1	1.213	1.206
O1–C–O2	125.4	125.6	C–O2	1.370	1.320
			O1–C–O2	122.4	121.9
MAD	0.018			0.020	
Compound	$CH_3CO_2CH_3$(**9**)[d]				
	Optimized structure	Crystal structure			
C–C	1.510	1.492			
C–O1	1.213	1.200			
C–O2	1.364	1.337			
$_{CH3CO2}$O2–C_{CH3}	1.446	1.453			
O1–C–O2	123.5	122.5			
MAD	0.016				

[a]The model compounds **1**, **2**, **3** and **6** show compartively high value of MAD which is attributed to the bulky substituents on P, Al, B and N-atoms in NHC in their crystal structures as compared to less bulky substituents in the model compounds.

[b] A. Albinati *Acta Cryst*., 1978, **B34**, 2188.

[c] P. G. Jonsson *Acta Cryst*., 1971, **B27**, 893.
[d] M. J. Barrow, S. Cradock, E. A. V. Ebsworth and D. W. H. Rankin *J. Chem. Soc., Dalton Trans.*, 1981, 1988.

Table S5: EDA-NOCV results for $CH_3COOC_2H_5$ (**10**) and $C_2H_5COOC_3H_7$ **(11)** at the BP86/TZ2P level of theory using ADF 2013.01 package. Energies are in kcal/mol

	$CH_3COOC_2H_5$ (**10**)			$C_2H_5COOC_3H_7$ **(11)**				
	$CH_3C—O_{CO2C2H5}$	$CH_3C^-\rightarrow O^+_{CO2C2H5}$	$CH_3CO_2O—C_{C2H5}$	$CH_3CO_2O^-\rightarrow C^+_{C2H5}$	$C_2H_5C—O_{CO2C3H7}$	$C_2H_5C^-\rightarrow O^+_{CO2C3H7}$	$C_2H_5CO_2O—C_{C3H7}$	$C_2H_5CO_2O^-\rightarrow C^+_{C3H7}$
ΔE_{int}	-104.9	-321.4	-105.0	-243.9	-101.7	-321.9	-121.3	-237.0
ΔE_{Pauli}	267.4	416.3	309.8	232.2	284.6	428.6	343.0	241.6
ΔE_{elstat} [a]	-161.4 (43.4%)	-374.8 (50.8%)	-153.9 (37.1%)	-248.8 (52.3%)	-172.6 (44.7%)	-378.8 (50.5%)	-167.5 (36.1%)	-244.9 (51.2%)
ΔE_{orb} [a]	-210.8 (56.6%)	-362.9 (49.2%)	-260.9 (62.9%)	-227.3 (47.7%)	-213.7 (55.3%)	-371.7 (49.5%)	-296.8 (63.9%)	-233.7 (48.8%)
ΔE_{σ} [b]	-185.0 (87.8%)	-303.0 (83.5%)	-232.5 (89.1%)	-182.2 (80.2%)	-186.7 (87.4%)	-311.3 (83.8%)	-270.5 (91.1%)	-185.8 (79.5%)
ΔE_{π} [b,c]	-9.8 (4.6%)	-16.2 (4.5%)	-12.1 (4.6%)	-15.5 (6.8%)	-9.9 (4.6%)	-16.1 (4.3%)	-13.1 (4.4%)	-15.0 (6.4%)
ΔE_{rest} [b,d]	16.0 (7.6%)	43.7 (12.0%)	16.3 (6.2%)	-29.6 (13.0%)	17.1 (8.0%)	44.3 (11.9%)	-13.2 (4.4%)	-32.9 (14.1%)
ΔE_{prep}	12.9	229.4	24.8	163.7	13.6	233.8	40.8	156.5
$\Delta E_{(-D_e)}$	-92.0	-92.0	-80.2	-80.2	-88.1	-88.1	-80.5	-80.5
$\Delta E_{orb}/\Delta E_{elstat}$	1.31	0.97	1.69	0.91	1.23	0.98	1.77	0.95

[a] Values in parenthesis give the percentage contribution to the total attractive interactions $\Delta E_{elstat} + \Delta E_{orb}$

[b] Values in parenthesis give the percentage contribution to orbital interaction ΔE_{orb}

[c] $\Delta E_{\mathbf{rest}} = \Delta E_{\mathbf{orb}} - (\Delta E_{\boldsymbol{\sigma}} + \Delta E_{\boldsymbol{\pi}})$

Table S6: Description of different bonding patterns depicted in Scheme 2.

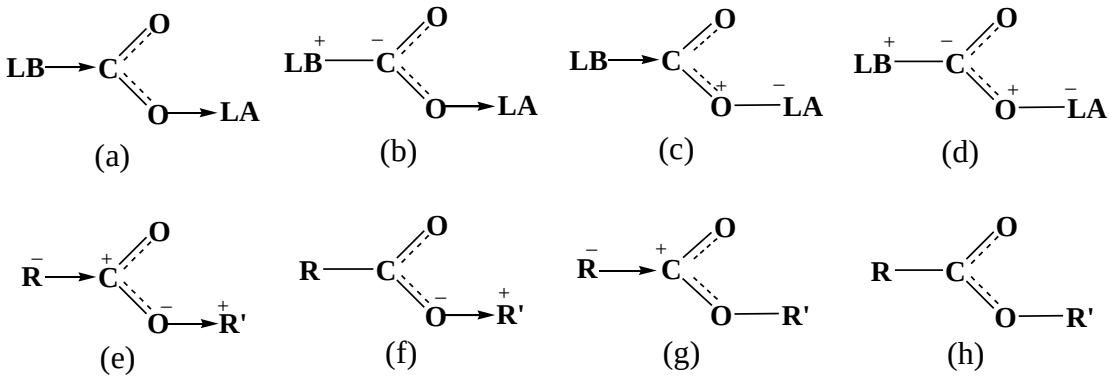

Here, we have explored the possibility of both electron sharing as well as donor-acceptor type bonding of CO_2 group with other fragments in **1-9** (Scheme 2). The appropriate formal charges are assigned to the corresponding fragments to maintain the correct electronic configuration. The bond formed between the LB and C-atom of CO_2LA can be of two types. The first possibility is the donor- acceptor interaction from the lone pair of LB to the empty orbital of the CO_2LA fragment (similar to the LUMO, $4a_1$ of bent CO_2, Figure 2), which is represented as $LB{\rightarrow}C_{CO2LA}$ in schemes 2a, c. The second possibility is the electron sharing ylidic-type interaction, which is represented as $LB^{+}–C^{-}_{CO2LA}$ in schemes 2b, d. The electronic state of the fragments involved in these schemes are formed by the transfer of one electron from the lone pair of LB to the empty orbital of CO_2LA (similar to the electronic state $^2A_1$ of bent CO_2^{-}, Figure 2), which results the formally positively charged LB^{+} and the negatively charged CO_2LA^{-} fragments.[16] In either way, once LB is bonded to the in-plane LUMO of bent CO_2 ($4a_1$), the in-plane π-MOs can reorganize as in-plane lone pair orbital on each O-atom. The O-atom can donate the lone pair to the empty orbital on LA, which is represented in schemes 2a, b. There may be another possibility that one electron from the lone pair on the O-atom (similar to $3b_2$, Figure 2) can be transferred to the vacant orbital on LA, which results LA^{-} and $LBCO_2^{+}$ fragments having unpaired electrons. The interaction of $LBCO_2^{+}$ and LA^{-} fragments results an ylidic type electron shairing $_{LBCO2}O^{+}–LA^{-}$ bond as shown in schemes 2c,d.

The bent CO_2 fragment should be in the excited electronic state ($^3B_2$, $1a_2^{2}3b_2^{1}4a_1^{1}$; Figure 2), where one electron from the HOMO ($3b_2$) is excited to the in-plane LUMO ($4a_1$), to form electron sharing $R–C_{CO2R'}$ and $_{RCO2}O–R'$ bonds as depicted in scheme 2h. The transfer of an electron from the singly occupied in-plane orbital on the CO_2R' fragment (similar to $4a_1$ of triplet

bent CO_2; Figure 2) to the singly occupied orbital of the R group results the formally negatively charged R^- and the positively charged $CO_2R'^+$ fragments, which can form donor-acceptor type $R^-\rightarrow C^+_{CO2R'}$ bond as shown in scheme 2g. On the other hand, transfer of an electron from the singly occupied in-plane orbital of the R′ group to the singly occupied orbital of the RCO_2 fragment (similar to $3b_2$ of triplet bent CO_2; Figure 2) results in the formally negatively charged RCO_2^- and the positively charged R'^+ fragment, which can form donor-acceptor type $_{RCO2}O^-\rightarrow R^+$ bond as shown in scheme 2f. If the electron transfer from the CO_2R' fragment to R group and R′ to CO_2R fragment happen at the same time, two donor-acceptor type $R^-\rightarrow C^+_{CO2R'}$ and $_{RCO2}O^-\rightarrow R'^+$ bonds would result as represented in scheme 2e.[16]